ISSN 1063-7729, Astronomy Reports, 2019, Vol. 63, No. 11, pp. 877–890. © Pleiades Publishing, Ltd., 2019.
Russian Text © The Author(s), 2019, published in Astronomicheskii Zhurnal, 2019, Vol. 96, No. 11, pp. 883–897.

Search for Fast Radio Bursts in the Direction of the Galaxies M31 and M33

V. A. Fedorova[1*] and A. E. Rodin[1]**

[1] *Pushchino Radio Astronomy Observatory, Astro Space Center, Lebedev Physical Institute, Pushchino, Moscow region, Russia*

Received February 22, 2019; revised May 14, 2019; accepted May 31, 2019

Abstract—The results of a search for individual fast radio bursts with the Large Phased Antenna of the Lebedev Physical Institute at 111 MHz during July 2012 through August 2018 are presented. The signals were distinguished by convolving the data with a template with a fixed form, followed by convolution with test dispersion measures. Areas of sky containing the galaxies M31 and M33 were chosen for the search. Three radio bursts were detected in the vicinity of M33, five in the vicinity of M31, and one in a region offset from the center of M31 by an hour in right ascension. The dispersion measures of the detected bursts range from 203 to 1262 pc/cm^3.

DOI: 10.1134/S1063772919110039

1. INTRODUCTION

Fast radio bursts (FRBs) are individual pulses with widths from 0.08 to 26 ms. They are likely extragalactic in origin, as is indicated, for example, by the fact that their dispersion measures usually range from 109 to ∼2600 pc/cm^3. Furthermore, there is no concentration of FRBs toward the Galactic plane in their distribution on the sky (as there is for pulsars) and there are no other distinguished directions in this distribution. According to data from the FRB catalog [1], about 100 FRBs are known. One of these, FRB 121102, has repeated a number of times from 2012 to the present time, at irregular time intervals. Thanks to these repeating bursts, it was possible to identify FRB 121102 with the vicinity of an irregular dwarf galaxy with active star formation [2]. This is the only FRB for which a host galaxy has been identified.

A second repeating burst was registered during a survey at 400 MHz using CHIME. Six repeating bursts with dispersion measures ∼189 pc/cm^3 and burst widths from 2.6 to 63 ms were registered from FRB 180814.J0422 + 73 during August–October 2018. Twelve new FRBs with various dispersion measures from 169.134 to 1006.84 pc/cm^3 were also detected in this survey [3].

Extragalactic FRBs have been known since 2007, when the first such burst was found by chance in archival data [4]. The first targeted attempts to detect extragalactic burst-like signals were made by Linscott and Erkes [5] in 1980. Subsequently, McCulloch et al. [6] carried out systematic observations of the Large Magellanic Cloud in 1980–1981 with the aim of searching for radio pulsars. Later, attempts were made to detect giant pulses from pulsars in various external galaxies, including M33, NGC253, NGC300, and NGC7793 [7]. In 2012, Rubio-Herrera et al. [8] carried out a search for burst signals in the galaxy M31. This led to the first detection of several bursts with dispersion measures corresponding to an extragalactic origin in the direction of M31.

The choice of relatively nearby galaxies for FRB searches was based on the idea that the objects giving rise to such bursts should be much more numerous in densely populated regions of the Universe, such as spiral galaxies. Two spiral galaxies in the Local Group, M31 and M33, fall in the field of view of the Large Phased Array (LPA) of the Pushchino Radio Astronomy Observatory. Accordingly, we selected these galaxies as targets for our FRB search.

Since there are a large number of theoretical models aiming to describe the origin of these mysterious events, we did not make any a priori assumptions about the nature of FRBs. We considered a purely observational problem—the detection of individual bursts displaying dispersion delays in frequency in the directions toward M31 and M33.

The observations were conducted at 111 MHz. This means that, for potentially detected radio bursts with dispersion measures of 10^2–10^3 pc cm^3, the pulse broadening in an individual channel with width

*E-mail: fedorova-astrofis@mail.ru
**E-mail: rodin@prao.ru

Table 1. Parameters of detected bursts

Date	Coordinates		DM, pc cm^{-3}	SNR	$F_{\max}$, Jy	E, Jy ms
	α	δ				
29.10.2012	0012	+42.06	732 ± 5	7.3	0.34	1380
30.10.2013	0025	+39.98	203 ± 4	10.1	0.24	800
12.02.2014	0131	+30.54	910 ± 4	9.2	0.26	945
16.12.2014	0014	+41.64	545 ± 5	7.6	0.23	1200
25.11.2015	0131	+30.98	273 ± 4	8.5	0.54	2450
28.11.2015	0132	+30.98	273 ± 4	7.2	0.52	2360
06.02.2016	0101	+41.63	1262 ± 5	7.9	0.26	1780
02.12.2016	2344	+40.80	291 ± 4	7.1	0.29	1320
21.03.2018	0033	+42.03	596 ± 5	8.2	0.54	2310

The coordinates are for epoch J2000, with α in hours and minutes and δ in degrees. DM is the dispersion measure, SNR the signal-to-noise ratio, $F_{\max}$ the peak flux density, and E the burst energy.

415 kHz should comprise a few to tens of seconds; i.e., the bursts being searched for should be very distorted by the dispersion delay and scattering. It is also obvious that such broadening will lead to a drop in the detection sensitivity by a factor of 10^3–10^4 for bursts with widths of several millseconds. In spite of this, astrophysical events with energies $>10^{46}$ J occurring in a nearby galaxy should be detectable.

Table 1 presents the parameters of nine new bursts we have detected in this study. The remaining sections of the paper describe the technical characteristics of the LPA, the observing and reduction method applied to archival data obtained during 2012–2018, and our results.

2. APPARATUS

The LPA of the Pushchino Radio Astronomy Observatory (PRAO) is one of the most sensitive radio telescopes operating at meter wavelengths. The operational frequency range of the LPA is 111 ± 1.25 MHz. The fluctuational sensitivity is 140 mJy for a time resolution of 0.1 s in a receiver bandwidth of 2.5 MHz [9]. The signals are registered using a multichannel digital receiver that enables recording in two regimes. In the first, the signal is written with relatively low frequency resolution using six frequency channels with bandwidths of 415 kHz each. In this mode, the time interval between readouts is 100 ms. This regime is used for continuous monitoring of scintillating sources. The second recording regime is carried out using 32 frequency channels with bandwidths of 78 kHz each, with a time resolution of 12.5 ms. Independent of the recording regime, the signal is reduced digitally using a 512-readout FFT processor. In our studies of the galaxies M31 and M33, we used data with a time resolution of 100 ms.

In connection with the specific features of the directional beam of the LPA, the effective area of the anntenna has its maximum value at the zenith (47 000 m^2) and decreases toward the horizon proportional to $\cos z$, where z is the zenith distance. The field of view of the radio telescope is ∼50 square degreees. This enables daily monitoring of a large number of sources. The system noise temperature depends on the sky background and varies from 550 to 3500 K.

A distinguishing characteristic of the LPA meridian radio telescope is its directional beam (DB), which includes a beam with an adjustable declination offset (DB-1) and a stationary beam (DB-3). DB-1 is used for studies of pulsars; the LPA has successfully been used to find pulsars by monitoring an appreciable fraction of the sky around the clock [10]. Observations with DB-3 can be carried out continuously. Since FRBs are sporadic events, our monitoring was conducted using DB-3, which has 96 sub-beams and was designed for studies of interplanetary scintillations of a large number of compact radio sources. The sub-beams cover the sky in declination from $-9°$ to $42°$. The half-width of the main DB-3 beam varies from $24'$ to $48'$, depending on the declination of the observed source.

M33 and M31 are extended sources, with angular sizes of $73' \times 45'$ (M33) and $3.2° \times 1°$ (M31). Such extended sources in the LPA field of view are covered by several sub-beams of the main DB. Since M31 has declination $\delta_{J2000} = 41.27°$, observations of this source were carried out using sub-beams 1–6 of

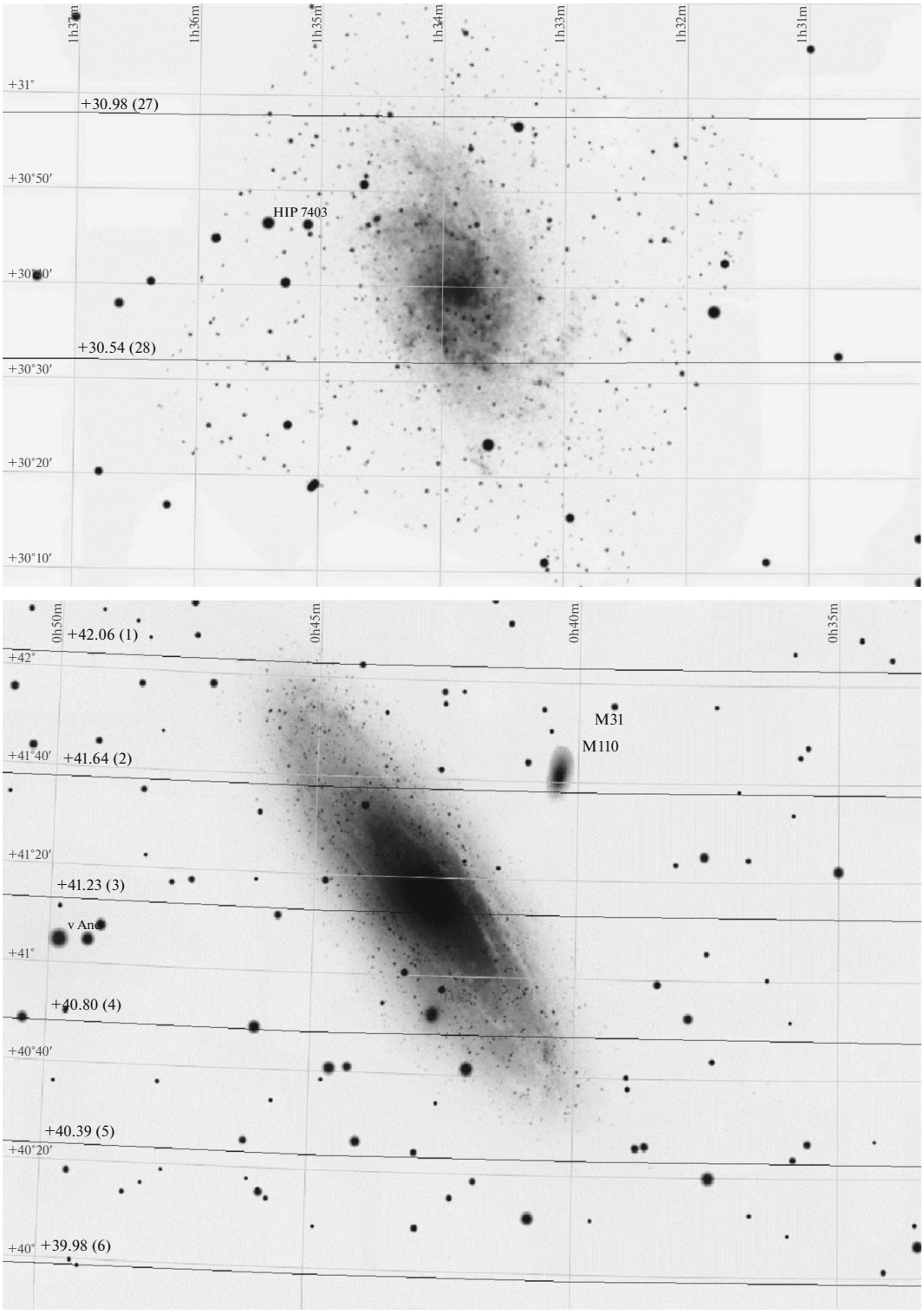

Fig. 1. The galaxies *M*33 (upper) and *M*31 (lower). The solid black lines show the declinations of the maxima of the LPA sub-beams. Each sub-beam is denoted using a coordinate and number corresponding to its location in the DB-3 directional beam of the LPA. The coordinates of the sub-beams and galaxies are given for epoch J2000.

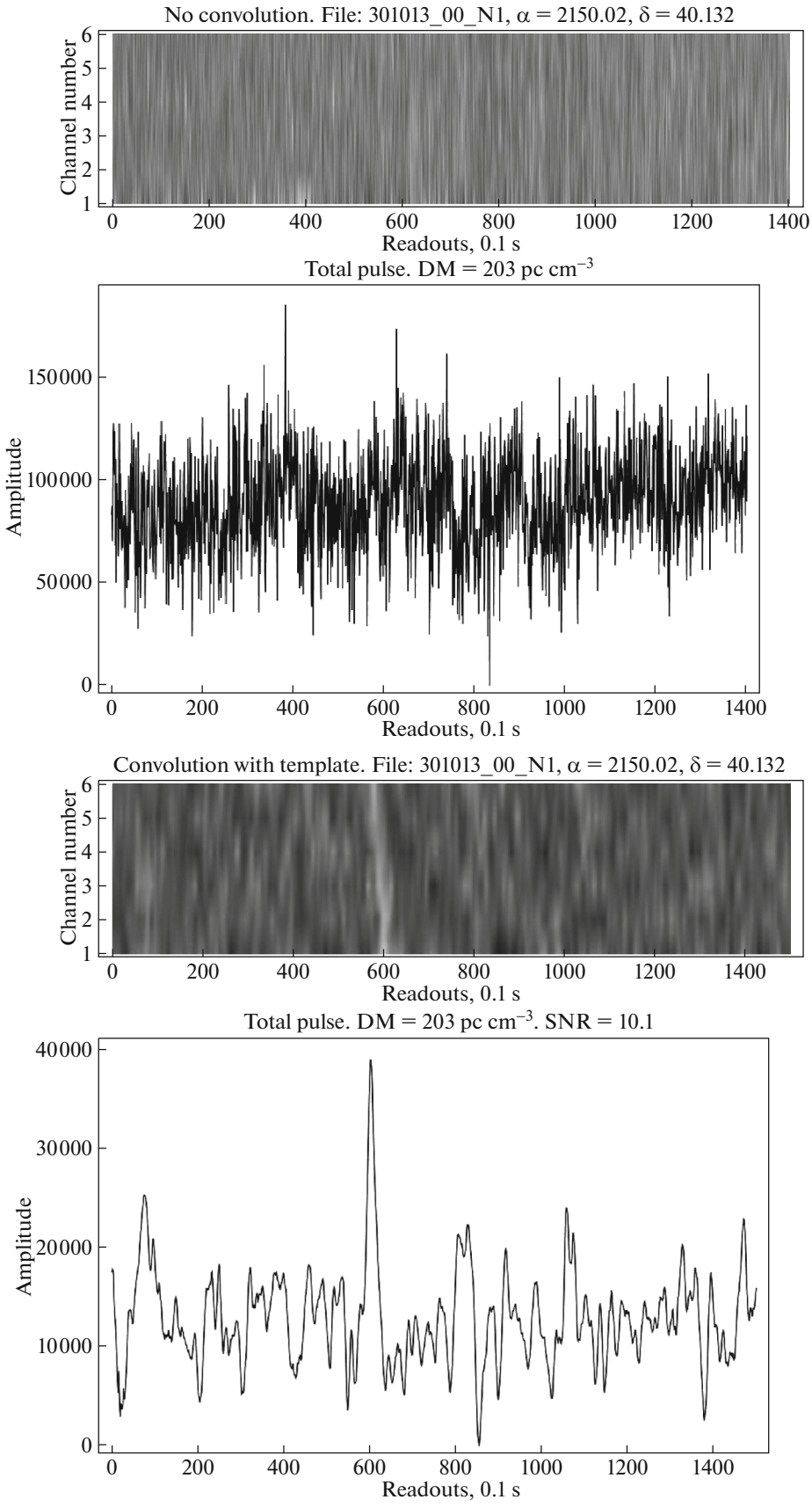

Fig. 2. LPA recording with a duration of 150 s corresponding to the FRB detected on October 30, 2013. The same section is shown without processing (upper two fragments) and after convolution with the template (lower two fragments).

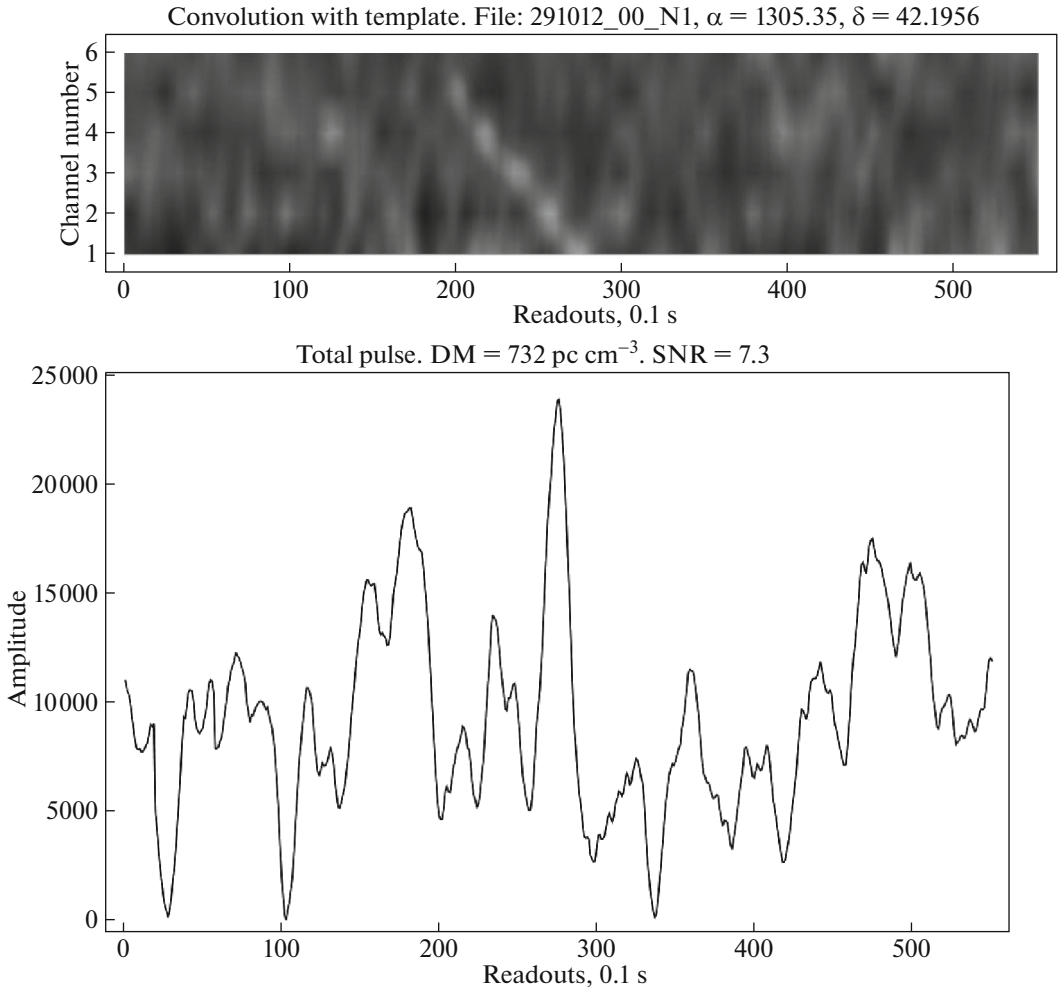

Fig. 3. Dynamical spectrum of the burst with $DM = 732$ pc/cm^3 detected on October 29, 2012. The lower image shows the total profile of the pulse. The peak flux density is 0.34 Jy. The Galactic coordinates are $l = 115.32°$, $b = -20.24°$.

DB-3. For M33, $\delta_{J2000} = 30.66°$, corresponding to observations using sub-beams 27 and 28 of DB-3. Figure 1 presents images of the studied galaxies in the optical together with the declinations of the DB-3 sub-beams.

The interference environment around the LPA is monitored regularly. Based on many years of measurements, several types of interference have been distinguished:

(1) atmospheric (lightning discharges, perturbatios of the ionosphere during solar flares);

(2) industrial (spark discharges from electrical instruments, passing automobiles, electric welding, and others);

(3) interference from radio equipment (television, VHF radio stations, radar, and others).

From the point of view of their effect on the LPA, all of these sources of interference have a common property: although they may be spatially localized, they influence the LPA receiver tract as a whole. This means that the interference signal arises simultaneously in several or even all sub-beams at the antenna output. There is no dependence of the arrival times of the interference signals on frequency (they exhibit zero dispersion measure) and interference is extended over time. This is true for both industrial interference and interference associated with solar ionospheric perturbations, which are registered in all sub-beams, and even in the antenna sidelobes. Thus, in contrast to terrestrial interference, a cosmic pulsed signal arrives from a specific direction on the sky and displays a frequency dependence for the arrival time.

Interference displaying frequency dependence of the arrival times, imitating a cosmic dispersion signal, is sometimes registered. However, in this case, the signal power exceeds the power of a cosmic signal

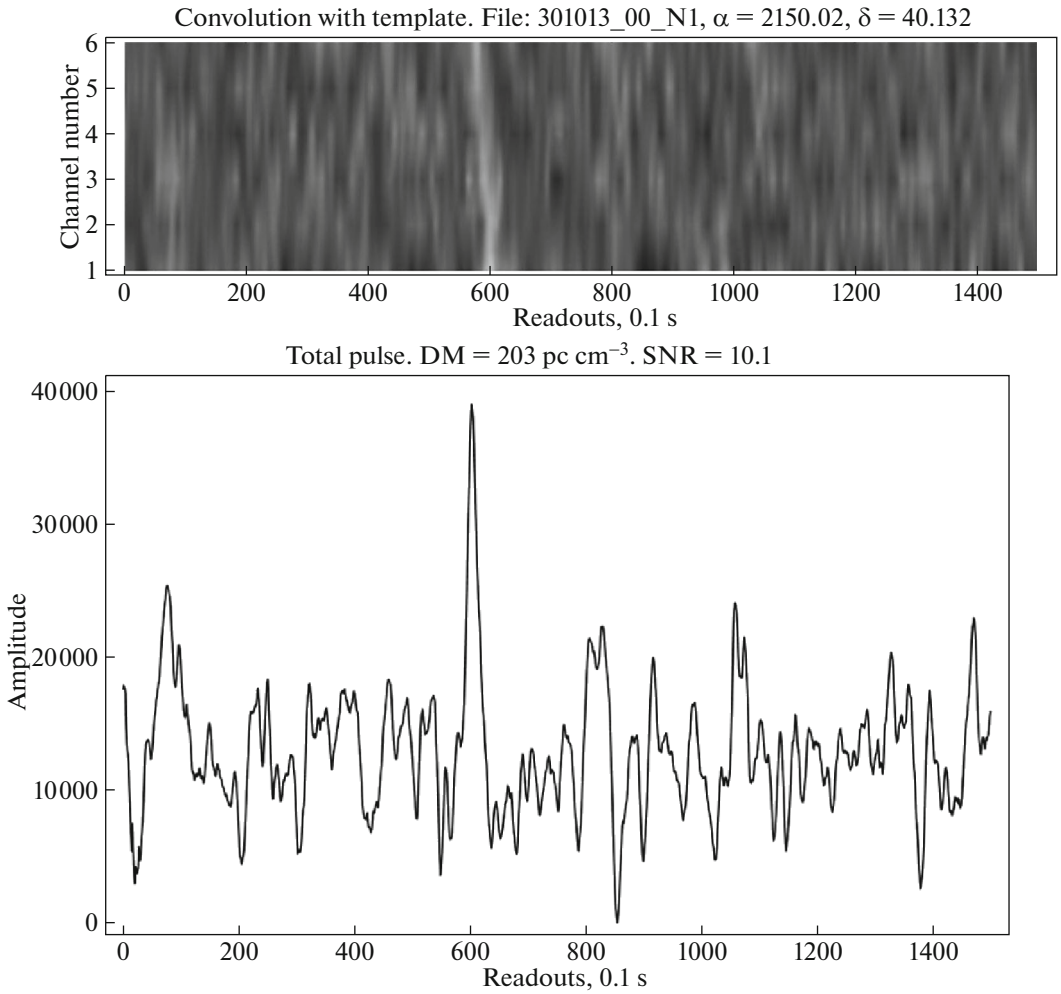

Fig. 4. Dynamical spectrum of the burst with $DM = 203$ pc/cm^3 detected on October 30, 2013. The lower image shows the total profile of the pulse. The peak flux density is 0.24 Jy. The Galactic coordinates are $l = 117.53°$, $b = -22.61°$.

very substantially, and the interference signal is registered in several sub-beams, making it easily distinguishable.

Overall, the interference environment worsens with the onset of Summer and the thunderstorm season, leading to an increase in the number of spurious signals in the data.

We considered pulses satisfying the following conditions to be candidate FRBs:

(1) visible in a single sub-beam,

(2) displaying a frequency dependence for the arrival times,

(3) registered in all six channels.

Pulses not satisfying these conditions were taken to be interference and were not considered to be candidate FRBs.

3. DATA REDUCTION

The data were reduced as follows. We used mathematical modeling to obtain the pulse-like signals expected for FRBs, taking into account their propagation in the interstellar medium and detection at low frequencies. Our modeling of the expected signals took into account the fact that the received burst differs from the emitted burst. The pulse shape is distorted by the influence of the inhomogeneous interstellar medium through which it propagates, and the resulting scattering t_s should be correlated with its dispersion measure DM. This correlation is described by Kuz'min et al. [11], and is given by $t_s = 0.06(0.01DM)^{2.2}$ at 110 MHz. In addition, the pulse undergoes a dispersion delay in frequency. The registration of the signal in a finite frequency band also leads to broadening, which is described by convolving the received signal with a Π-like function:

$$\Pi(t) = \sigma(t - \tau_{i-1})\sigma(\tau_i - t), \qquad (1)$$

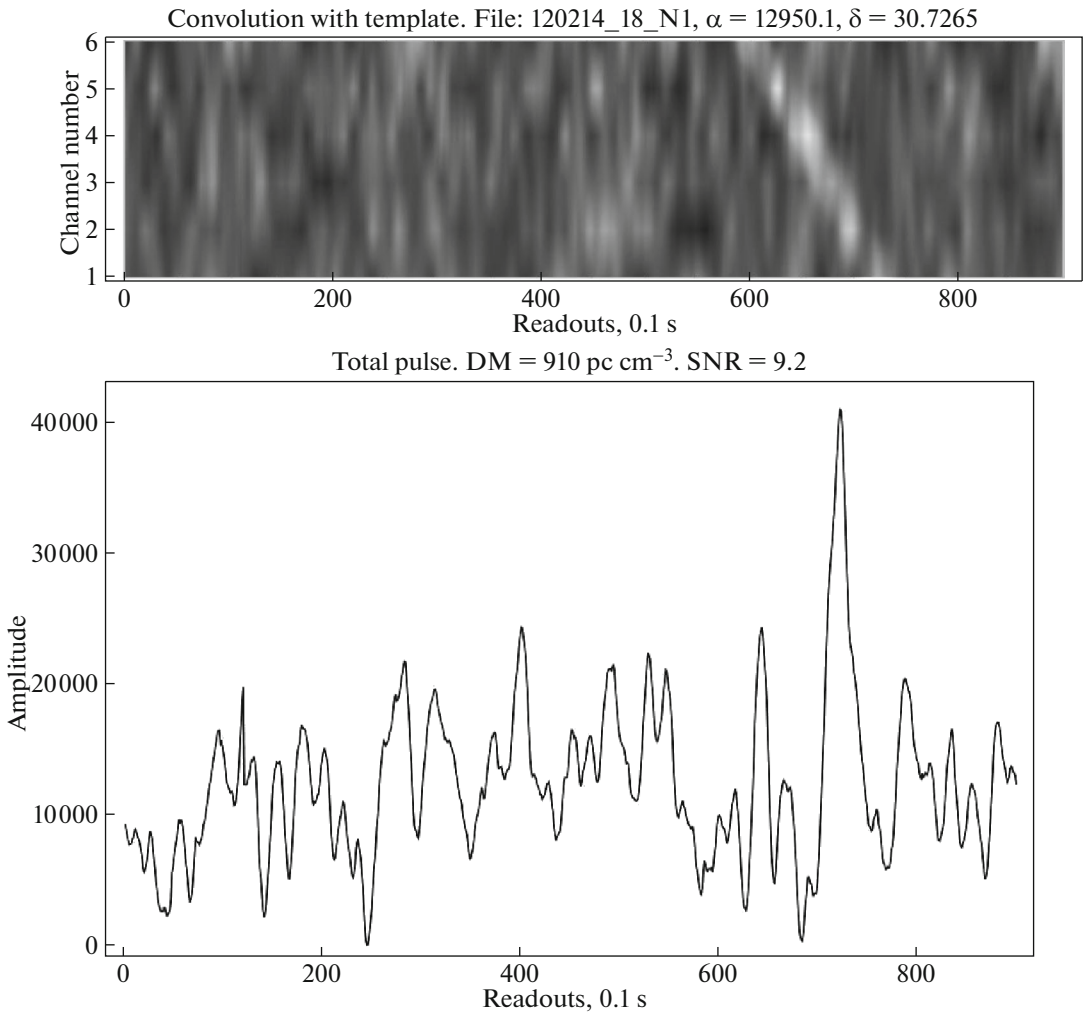

Fig. 5. Dynamical spectrum of the burst with $DM = 910$ pc/cm^3 detected on February 12, 2014. The lower image shows the total profile of the pulse. The peak flux density is 0.26 Jy. The Galactic coordinates are $l = 133.10°$, $b = -31.54°$.

where $\sigma(t)$ is a single step function and τ_i is the arrival time at the boundary of frequency channel i. The quantity $\Delta\tau = \tau_i - \tau_{i-1}$ $(i = 1, 2, 3, \ldots, 6)$ is the broadening of the pulse within the band. To distingish impulsive dispersion signals, we convolved a pulse containing noise with a template applying dispersion compensation, making it possible to obtain the maximum signal-to-noise ratio (SNR). The process used to conduct the modeling and obtain the template is described in detail in [12].

The method used to search for FRBs was as follows. We first analyzed the daily recordings in the six frequency channels with a time resolution of 0.1 s in sub-beams coinciding with the directions toward M31 and M33. We then applied corrections taking into account the deviation of the LPA sub-beams from the plane of the celestial meridian and precession. For M33, in sub-beams 27 and 28, we selected the five-minute section from an hourly recording corresponding to the right ascension of M33 ($\alpha_{J2000} = 01^{\rm h}34^{\rm m}$). In the case of M31, we chose a half-hour section of a recording in the first six sub-beams, with their center corresponding to the right ascension of the center of M31 $\alpha_{J2000} = 00^{\rm h}43^{\rm m}$. Further, we convolved the recordings in each sub-beam with a template obtained through our mathematical modeling, after which we convolved the resulting signal with test dispersion measures ranging from 0 to 3000 pc/cm^3 in steps of 50 [12].

Since FRBs manifest as weak individual pulses at 111 MHz, due to their appreciable scattering and broadening, it is not possible to directly detect these signals without applying additional methods such as we have used. Our approach implementing convolution with a template with an appropriate form makes it possible to amplify the burst signal against the noise background. As an example of the operation of the method, Fig. 2 presents the same section of recording before and after convolution with the template.

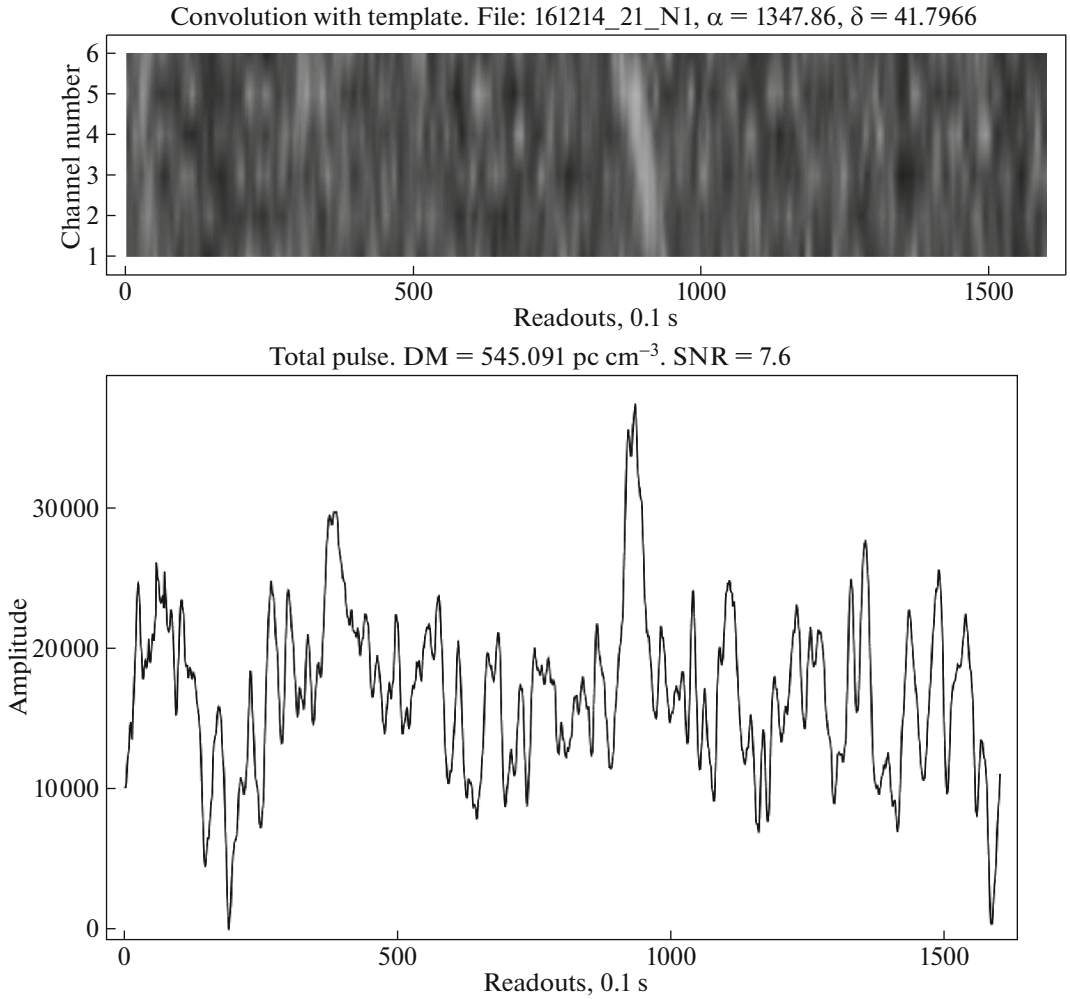

Fig. 6. Dynamical spectrum of the burst with $DM = 545$ pc/cm^3 detected on December 16, 2014. The lower image shows the total profile of the pulse. The peak flux density is 0.23 Jy. The Galactic coordinates are $l = 115.55°$, $b = -20.70°$.

The subsequent processing of the data amounted to a visual analysis of the results obtained in the last stage of the reduction. When a burst signal was detected, the dispersion measure, peak flux density, and SNR were determined separately in each case. The results are presented in Table 1.

4. RESULTS

Our visual analysis of the data led to the detection of nine FRBs with dispersion measures from 203 to 1262 pc/cm^3 (see Figs. 3–11). One of these may have repeated, as is suggested by two bursts with coordinates coincident within the half-width of the LPA direction beam and displaying dispersion measures coincident to within ±4 pc/cm^3. These tentatively repeating bursts were registered several days apart (November 25, 2015 and November 28, 2015).

The SNR values for the registered bursts after applying a matched filter were all $\lesssim$10, indicating that the peak flux densities for the registered bursts given in Table 1 are at the limit of the antenna sensitivity. Note also that we distinguish only the upper part of the burst with our method, since the lower, exponentially decaying, part is lost in the noise.

The burst registered on March 21, 2018 (Fig. 10) merits special attention. The main signal is clearly visible in the dynamical spectrum, however another pulse can be noted to the right of the main pulse after ~300 readouts. The second pulse is clearly visible in the right-hand part of the total recording for six frequency channels. This event is of special interest and requires further more detailed study.

Table 1 also presents the right ascension corresponding to the sixth frequency channel ($f =$ 111.5 MHz) and the estimated SNR.

The dispersion measures of Galactic pulsars range from ~3 to ~1800 pc/cm^3 for pulsars in the direction of the Galactic center, which fully covers the range of dispersion meaures for our detected FRBs. Some of

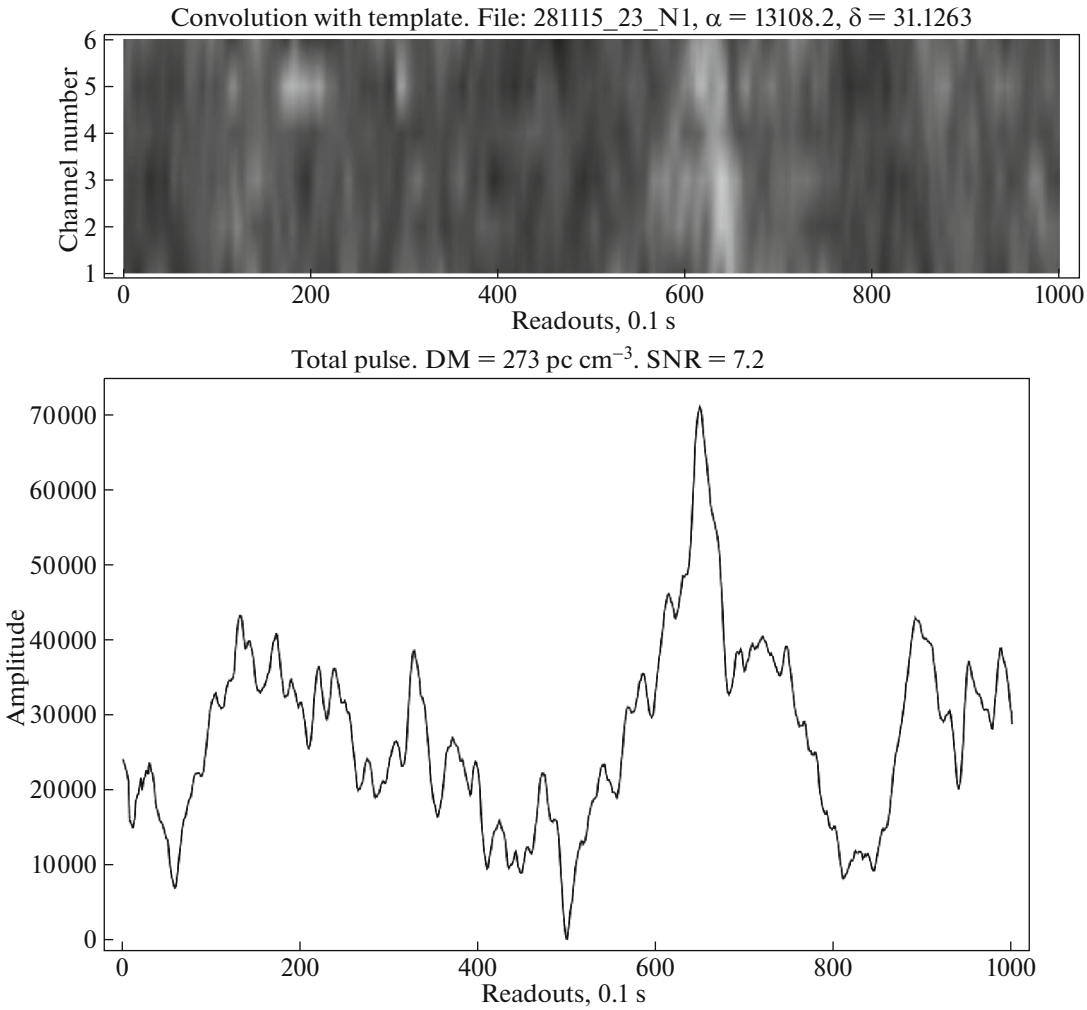

Fig. 7. Dynamical spectrum of the burst with $DM = 273$ pc/cm^3 detected on November 28, 2015. The lower image shows the total profile of the pulse. The peak flux density is 0.54 Jy. The Galactic coordinates are $l = 133.20°$, $b = -31.07°$.

the detected pulses with high DM values are far from the optically bright parts of M31 and M33, where the concentration of matter is appreciably lower than in the central regions. This suggests that, since a sufficient amount of matter to explain the observed DM values is not accumulated in the regions where the bursts are located, not all the bursts are associated with the two galaxies studied, and more likely coincide with the directions of these galaxies by chance.

The presence of noise in the recordings on some days could suggest that the detected bursts could form by chance due to the superposition of intensity variations at "needed" places in the recordings in the six frequency channels. Therefore, we decided to subject the results obtained to a detailed statistical analysis. This analysis was carried out in two ways: we calculated the probability of a chance alignment of the pulses to form the dynamical spectra and the probability that the burst arose by chance, as functions of the SNR.

Recall that we analyzed daily recordings with durations of $T_{\rm rec} = 300$ s. Each recording was passed through a matched filter with characteristic width $t_s = 1$ s, leading to $m = T_{\rm rec}/t_s$ independent readouts in the recording. Figure 12 schematically shows the dynamical spectrum with all quantities used. We introduced the quantity $k = t_{\rm pulse}/t_s$. The widths of the detected pulses $t_{\rm pulse}$ are several seconds, yielding $k \sim 1{-}5$. We also introduced the quantity $p = T_{\rm rec}/t_{\rm pulse}$. The probability that readings in one channel line up, forming a pulse, is $P_m = 1/[(m{-}1)(m{-}2)...(m{-}k)]$. The probability that individual bursts in channels form the dynamical spectrum is $P_n = 1/p^{(n-1)}$, where $n = 6$ is the number of frequency channels. The -1 in the power-law index in the denominator for the probability P_n takes into account the fact that a pulse can appear in any place in a recording, and that this does not affect the fact of a detection. Thus, the overall probability that

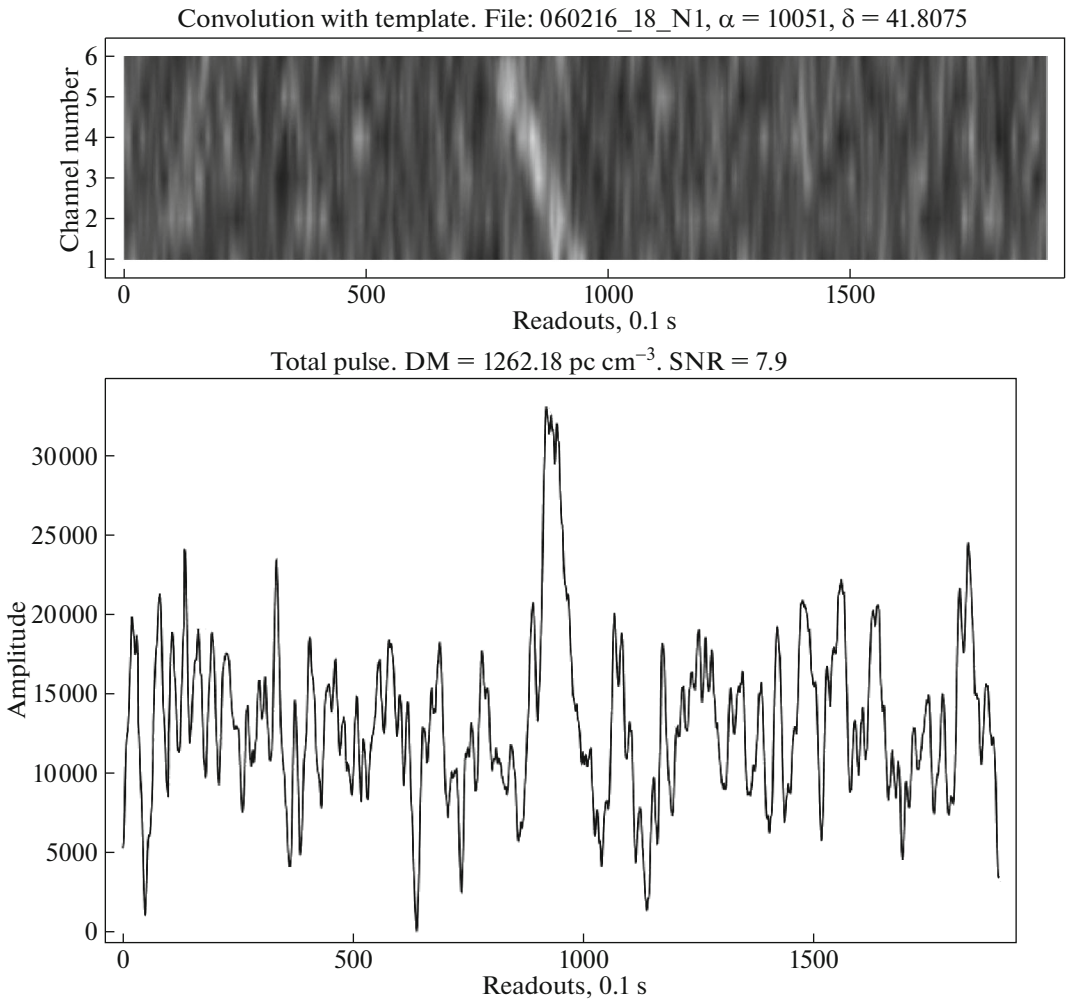

Fig. 8. Dynamical spectrum of the burst with $DM = 1262$ pc/cm^3 detected on February 6, 2016. The lower image shows the total profile of the pulse. The peak flux density is 0.26 Jy, The Galactic coordinates are $l = 124.90°$, $b = -21.20°$.

the readouts align to form the observed dynamical spectrum by chance is $P_{\rm tot} = P_m P_n \sim 10^{-12}$–$10^{-19}$.

The probability that a readout exceeds a threshold SNR was calculated as follows. We subtracted mean values smoothed over 150 readouts obtained using a median filter from the recordings in each channel. We further constructed the empirical distribution of the readouts. This distribution was best described by a Laplace (double exponential) distribution. We determined the parameters of the distribution (its mean and dispersion), and used these parameters to calculate the probability of exceeding a specified SNR. This probability proved to be $P_r = 3 \times 10^{-2}$–8×10^{-3} for SNR ~ 7–10.

Thus, the detection of FRBs reduces to simultaneously satisfying two conditions: the readings exceeding a threshold SNR and alignment of these readings to form the dynamical spectrum. The probability that both of these conditions are satisfied simultaneously by chance is $P = P_r P_{\rm tot} \sim 10^{-14}$–$10^{-23}$; in our view, this is too low to occur by chance in 6930 hrs of analyzed data in ∼82 000 individual scans.

5. DISCUSSION

Our primary aim was to search for and estimate the parameters of FRBs in the directions of the galaxies M31 and M33 in archival LPA data. The estimated dispersion measures for the detected bursts presented in Table 1 and the absence of a visible concentration of the bursts toward the centers of the two galaxies studied lead to the natural suggestion that the regions in which some bursts were generated are located far beyond these galaxies. Thus, we conclude that M31 and M33 are not the host galaxies for all the registered burst signals.

We registered similar bursts in other parts of the sky earlier [13]. The characteristics of our newly detected signals are similar to those of the pulses

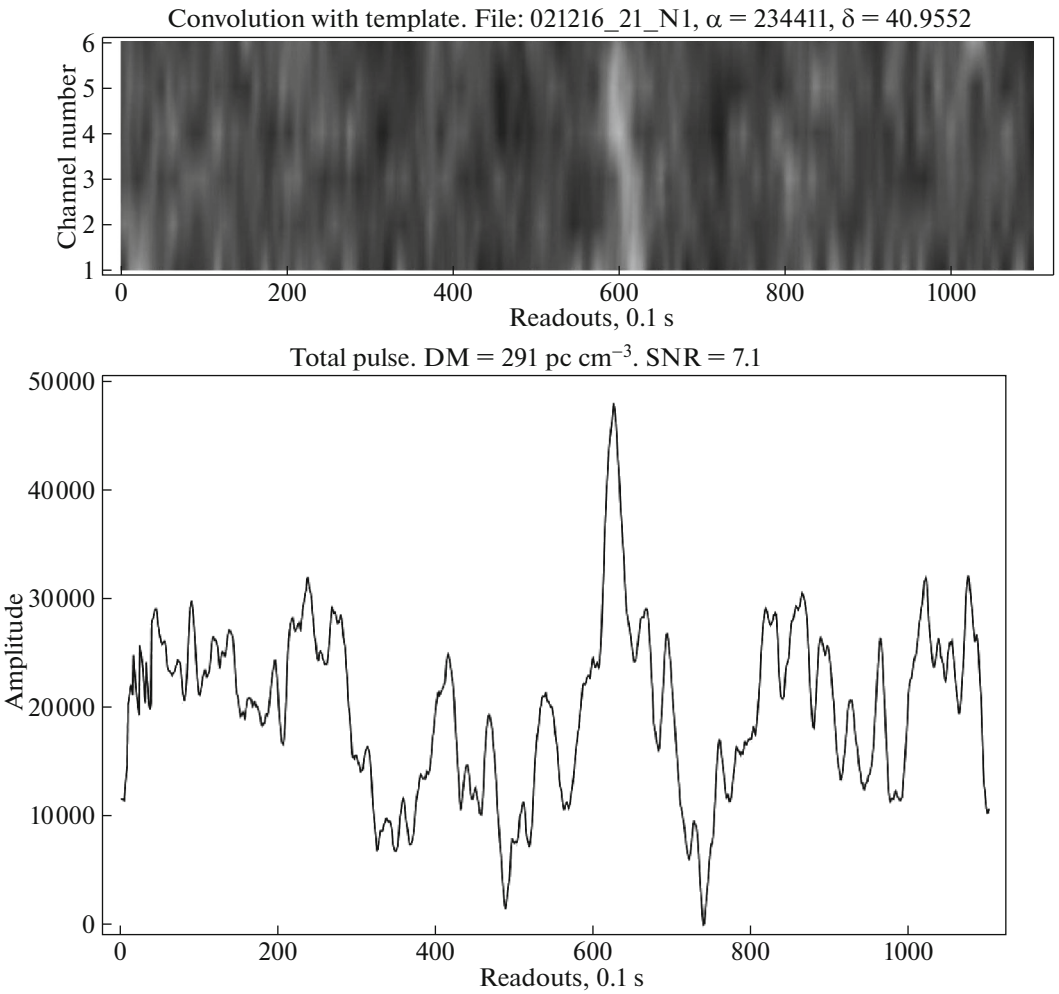

Fig. 9. Dynamical spectrum of the burst with $DM = 291$ pc/cm^3 detected on December 2, 2016. The lower image shows the total profile of the pulse. The peak flux density is 0.29 Jy. The Galactic coordinates are $l = 109.48°$, $b = -20.32°$.

reported in [12], and also to the cataloged parameters of FRBs.

We separately touch on the question of the observed number of radio bursts. A region of sky covering ∼30 square degrees observed over six years was analyzed. Over this time, nine bursts were detected. Recalculating this number to the entire area of the sky and supposing that the detected bursts are not associated with the galaxies M31 and M33, we obtain a mean burst detection rate for the LPA at 110 MHz of ∼2000 bursts/year.

At present, one problem with studies of these events is estimates of their spectral indices. Estimates of this quantity for FRB 121102 in various articles range from 1 to 10 [14]. In our view, this large scatter in the deduced spectral indices can be explained mainly by the fact that these measurements were carried out in a receiver bandwidth in which the instantaneous frequency distribution of the peak flux density is determined by scintillation as the pulse propagates in the interstellar medium, not physics associated with the radiation itself. After detecting a large number of new bursts from FRB 121102 during 2018, Macquart et al. [15] derived the spectral index $\alpha = -1.6$. In [16], we reported the spectral index for FRB 121102 $\alpha \sim -0.6 \pm 0.4$. This result was based on an analysis of measured flux densities for the repeating radio burst FRB 121102 and on our suggestion [12] that we registered and measured a repeat pulse from this object at 111 MHz.

Egorov and Postnov [17] proposed a mechanism for the generation of radio bursts based on the interaction of a plasma flow streaming out from the magnetic poles of a neutron star and a shock that arises after the SN explosion and passes by the pulsar. At present, this is not generally considered to be the main mechanism at work, since it does not explain accompanying behavior in other ranges or repeating radio bursts. Nevertheless, the idea of the "ignition" of matter by a cone of radiation from a pulsar

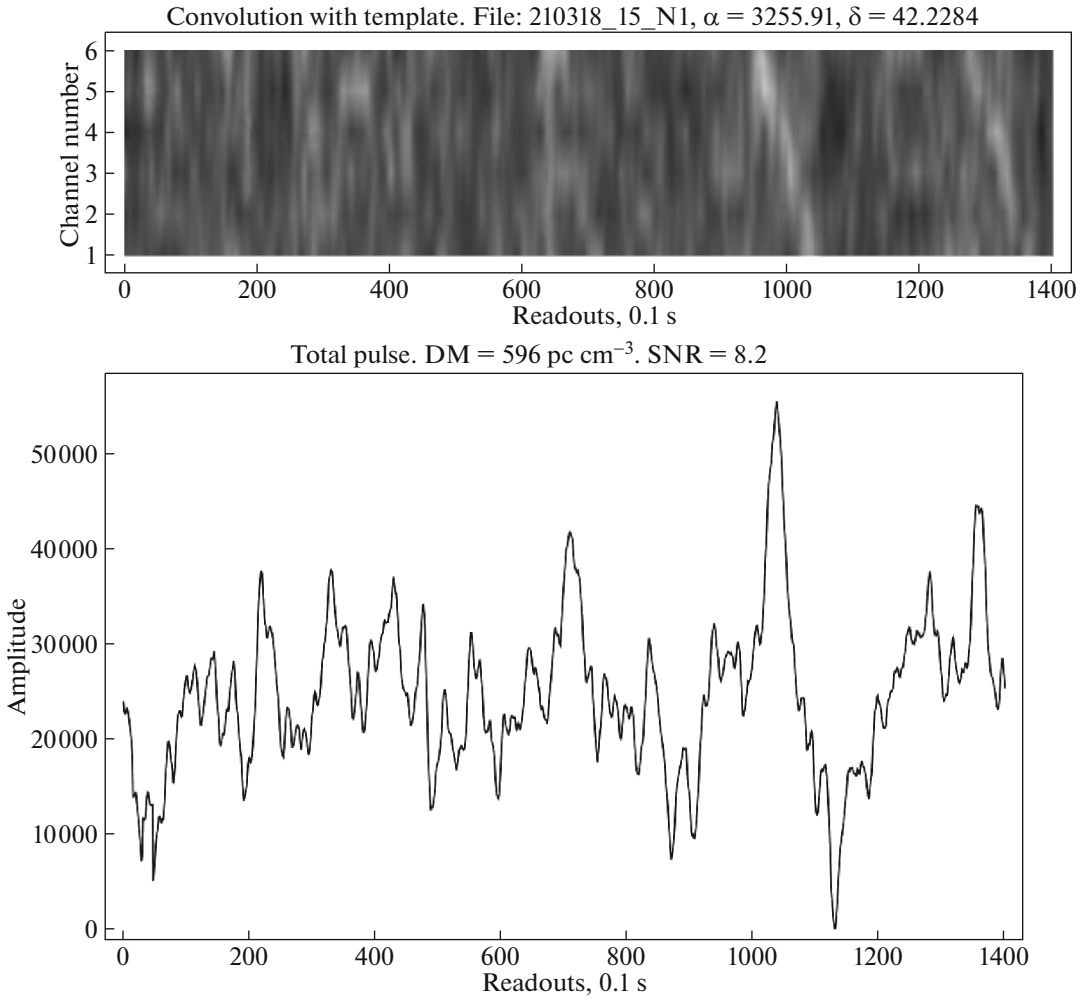

Fig. 10. Dynamical spectrum of the burst with $DM = 596$ pc/cm^3 detected on March 21, 2018. The lower image shows the total profile of the pulse. The peak flux density is 0.54 Jy. The Galactic coordinates are $l = 119.46°$, $b = -20.72°$.

is interesting. If we consider a hypothetical binary system with a pulsar in which the stellar companion displays activity in the form of matter ejections, this mechanism will give rise to radio bursts at irregular time intervals.

We also wish to mention an idea concerning the high dispersion measures of radio bursts. Depending on the relative geometry for the shock, neutron star, and observer, a situation can arise when a pulse must pass through a substantial thickness of ionized matter. In turn, this leads to high values for the observed DM. In this case, the inferred distances at which radio bursts are believed to arise and the deduced burst energies must both be lowered.

Returning to the question of modeling the events generating FRBs, we propose the following.

First, of the entire list of FRBs, two stand out: FRB 121102 and FRB 180814.J0422+73. Their pulses were detected more than once, in contrast to the others. This already suggests that repeating and non-repeating FRBs are generated by different mechanisms.

Second, a visual analysis of the registered FRBs shows that they have very different appearances, in particular, different widths, which cannot be epxlained purely by broadening in the receiver bandwidth and are associated with internal properties of the pulses.

Third, the high dispersion measures DM and estimated energies of all these events may indicate that we are dealing with a fundamentally new phenomenon that is not yet known or has been predicted only theoretically. Possibilities include, for example, the model proposed in [18], in which the Primakov process is used to explain the transformation of axions—dark matter particles—into photons in a magnetic field. Note that the disruption of clouds of such matter by an object with a powerful magnetic

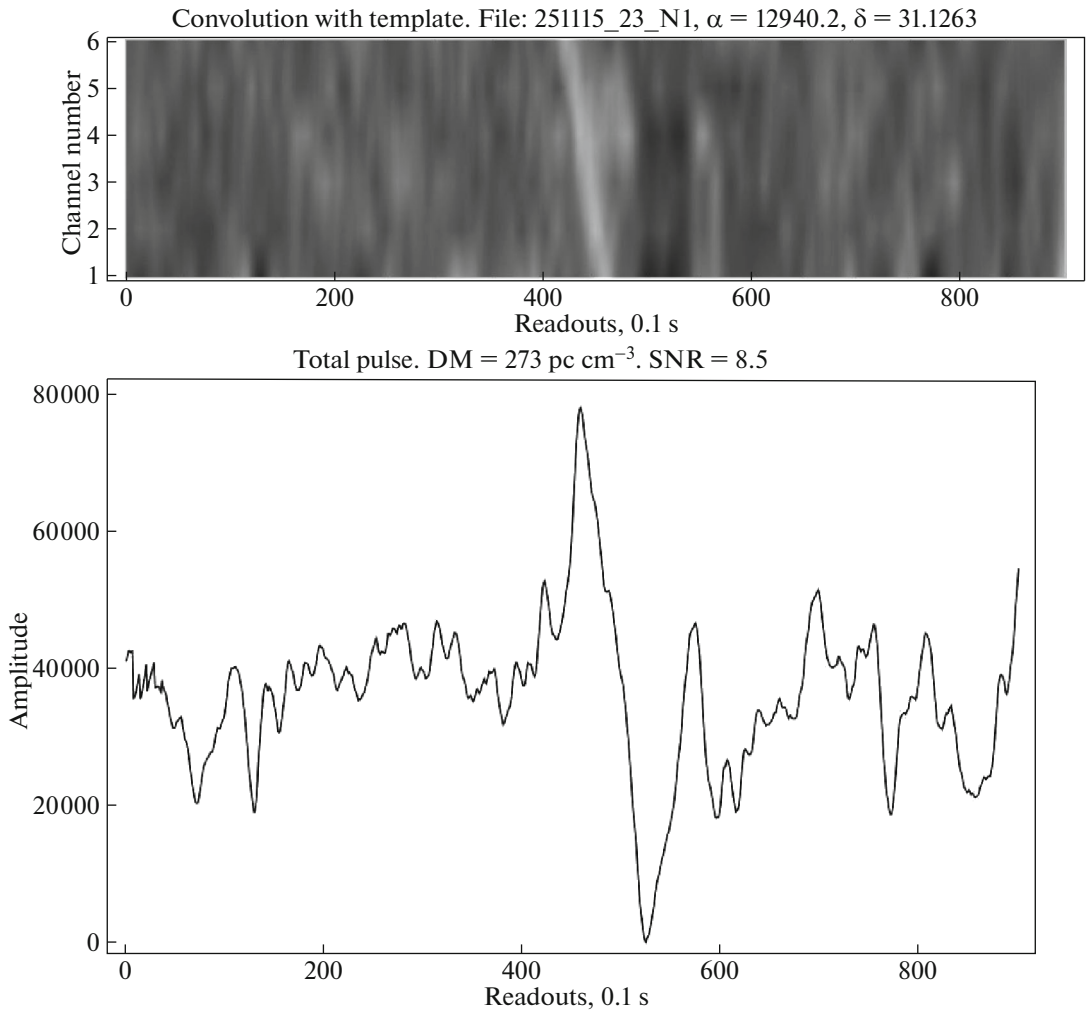

Fig. 11. Dynamical spectrum of the burst with $DM = 273$ pc/cm^3 detected on November 25, 2015. The lower image shows the total profile of the pulse. The peak flux density is 0.54 Jy. The Galactic coordinates are $l = 133.02°$, $b = -31.10°$.

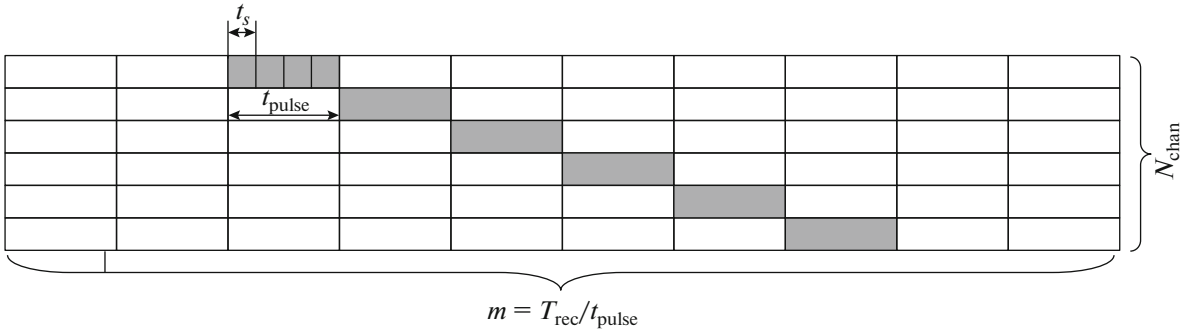

Fig. 12. Schematic image of the dynamical spectrum for computation of the probability of appearance by chance. $T_{rec} = 300$ s is the duration of the recording, $N_{chan} = 6$ the number of frequency channels, $t_s = 1$ s the scattering for the template, and t_{pulse} the characteristic pulse width.

field could generate pulses with durations of several seconds [19]. All the detected bursts have characteristics widths of several seconds. Compensation for scattering in the medium and broadening in the frequency channels can reduce the burst widths to ~0.1–2 s.

Thus, in spite of the existence of models that can explain both individual and repeating FRBs, we find

the possibility that these two types of events have different natures more natural.

6. CONCLUSION

Our main results follow.

1. We have detected three FRBs in the direction of M33 in archival LPA data obtained from July 2012 through August 2018, two of which tentatively arose in the same region on the sky and thus may represent a repeating FRB.

2. In this same period, we detected six FRBs with various dispersion measures in the direction of M31.

Thus, in all, we detected nine FRBs with dispersion measures ranging from 203 to 1262 pc/cm^3 in archival LPA data for the period from July 2012 though August 2018. All the parameters of these bursts are presented in Table 1.

ACKNOWLEDGMENTS

We thank the Director of the Pushchino Radio Astronomy Observatory R.D. Dagkesamanskii and the Assistant Director V.V. Oreshko for discussions of this paper that have led to its improvement.

FUNDING

V. A. Fedorova was partially funded by the Russian Foundation for Basic Research (grant 16-29-13074).

REFERENCES

1. E. Petroff, L. Houben, K. Bannister, S. Burke-Spolaor, et al., arXiv:1710.08155 [astro-ph.IM] (2017).
2. M. Kokubo, K. Mitsuda, H. Sugai, S. Ozaki, et al., Astrophys. J. **844**, 95 (2017).
3. M. Amiri, K. Bandura, M. Bhardwaj, P. Boubel, et al., Nature **566**, 230 (2019).
4. D. R. Lorimer, M. Bailes, M. A. McLaughlin, D. J. Narkevic, and F. Crawford, Science **318** (5851), 777 (2007).
5. I. R. Linscott and J. W. Erkes, Astrophys. J. **236**, L109 (1980).
6. P. M. McCulloch, P. A. Hamilton, J. G. Ables, and A. J. Hunt, Nature **303**, 307 (1983).
7. M. A. McLaughlin and J. M. Cordes, Astrophys. J. **596**, 982 (2003).
8. E. Rubio-Herrera, B. W. Stappers, J. W. T. Hessels, and R. Braun, Mon. Not. R. Astron. Soc. **428**, 2857 (2013).
9. V. V. Oreshko, G. A. Latyshev, I. A. Alekseev, Yu. A. Azarenkov, B. I. Ivanov, V. M. Karpov, and V. I. Kastromin, Tr. IPA **24**, 80 (2012).
10. A. E. Rodin, V. V. Oreshko, and V. A. Samodurov, Astron. Rep. **61**, 30 (2017).
11. A. D. Kuz'min, B. Ya. Losovskii, and K. A. Lapaev, Astron. Rep. **51**, 615 (2007).
12. V. A. Fedorova and A. E. Rodin, Astron. Rep. **63**, 39 (2019).
13. A. E. Rodin, V. A. Fedorova, V. A. Samodurov, and S. V. Logvinenko, Astron. Tsirk. **1641**, 1 (2018).
14. L. G. Spitler, J. M. Cordes, W. T. Hessels, D. R. Lorimer, et al., Astrophys. J. **790**, 101 (2014).
15. J.-P. Macquart, R. M. Shannon, K. W. Bannister, C. W. James, R. D. Ekers, and J. D. Bunton, arXiv:1810.04353 [astro-ph.HE] (2018).
16. A. E. Rodin and V. A. Fedorova, Astron. Telegram, No. 11932, 1 (2018).
17. A. E. Egorov and K. A. Postnov, Astron. Lett. **35**, 241 (2009).
18. I. I. Tkachev, JETP Lett. **101**, 1 (2015).
19. M. S. Pshirkov, Int. J. Mod. Phys. D **26**, 1750068 (2017).

Translated by D. Gabuzda